



Article

Practical Operation Strategies for Energy Storage System under Uncertainty

Minsoo Kim ¹, Kangsan Kim ¹, Hyungeun Choi ¹, Seonjeong Lee ²  and Hongseok Kim ^{1,*} 

¹ Department of Electronic Engineering, Sogang University, Baekbeom-ro 35, Mapo-gu, Seoul 04107, Korea; youngjae6@sogang.ac.kr (M.K.); ks12000@sogang.ac.kr (K.K.); hyungeun@sogang.ac.kr (H.C.)

² Encored Technologies, Bongeunsa-ro 215, Kangnam-gu, Seoul 06109, Korea; sjlee@encoredtech.com

* Correspondence: hongseok@sogang.ac.kr; Tel.: +82-2-705-7989

Received: 27 February 2019; Accepted: 18 March 2019; Published: 21 March 2019



Abstract: Recent advances in battery technologies have reduced the financial burden of using the energy storage system (ESS) for customers. Peak cut, one of the benefits of using ESS, can be achieved through proper charging/discharging scheduling of ESS. However, peak cut is sensitive to load-forecasting error, and even a small forecasting error may result in the failure of peak cut. In this paper, we propose a two-phase approach of day-ahead optimization and real-time control for minimizing the total cost that comes from time-of-use (TOU), peak load, and battery degradation. In day-ahead optimization, we propose to use an *internalized pricing* to manage peak load in addition to the cost from TOU. The proposed method can be implemented by using dynamic programming, which also has an advantage of accommodating the state-dependent battery degradation cost. Then in real-time control, we propose a concept of *marginal power* to alleviate the performance loss incurred from load-forecasting error and mimic the offline optimal battery scheduling by learning from load-forecasting error. By exploiting the marginal power, real-time ESS charging/discharging power gets close to the offline optimal battery scheduling. Case studies show that under load-forecasting uncertainty, the peak power using the proposed method is only 22.4% higher than the offline optimal peak power, while the day-ahead optimization has 76.8% higher peak power than the offline optimal power. In terms of profit, the proposed method achieves 77.0% of the offline optimal profit while the day-ahead method only earns 19.6% of the offline optimal profit, which shows the substantial improvement of the proposed method.

Keywords: energy storage system (ESS); optimal scheduling; peak cut; battery degradation; internalized pricing; forecasting error; marginal power

1. Introduction

Recent developments of battery technologies have made battery prices drop sharply, and thus individual customers actively deploy the energy storage system (ESS) to minimize electricity cost considering time-varying electricity price and renewable generation such as solar and wind power. ESS is also beneficial from a power system point of view, since it contributes to stabilizing the power grid. Thus, there have been many studies to minimize total electricity cost using ESS [1–8].

In minimizing total cost using ESS, energy management system needs to consider several factors such as load profiles, peak power, country-specific tariff, and time-of-use (TOU) pricing. In the literature, the ESS operation problem is formulated to have a linear objective function, and the solution can be obtainable using linear programming [2]. Please note that peak cut requires min-max operation, and linear programming can be used for this purpose [3]. In case operational constraints include binary decision variables, mixed-integer linear programming was used [4]. Recently, to extend battery

lifetime, the authors in [7] considered the state-dependent battery degradation cost and applied dynamic programming because linear programming is not effective for developing state-dependent policies.

The works in [2,4,7], however, assumed that short-term load-forecasting is error-free. Indeed, peak cut using ESS is challenging because of the uncertainty of load profile, and it is known that peak cut may be vulnerable to load-forecasting error [3,9]; even if there is small load-forecasting error, the peak power originated both from the load and ESS operation can significantly vary. This is because battery scheduling for peak cut depends on the forecasted load profile [5], and small forecasting error may cause another unwanted peak power. Strategies for managing peak power may differ from countries to countries; for example, under Korea commercial and industrial (KCI) tariff, the peak power measured for 15 min determines the monthly *base* cost, and it may affect up to the next 12 months [3]. Thus, managing peak power is of prime importance under KCI tariff. Since the charging and discharging scheduling of ESS is typically done day-ahead, under the presence of forecasting error, day-ahead scheduling can be problematic, specifically for managing peak load. To mitigate the adverse impact of forecasting error on peak cut, the authors in [3] use robust optimization and propose to reserve some portion of ESS. Robust optimization, however, can be too conservative because it is mainly focused on handling the worst case. In addition, it is not clear how much to reserve for robust operation [3]. Chance constrained programming (CCP) alleviates the conservativeness of the robust optimization [10,11]. CCP uses the uncertainty with certain probability as constraints. Obtaining the probability, however, is challenging in real situations. The work in [8] generates hourly forecasted load by probabilistic load distribution to alleviate the uncertainty. However, the authors in [8] assume that the probabilistic load distribution follows the normal distribution, which may not necessarily hold in general. Scenario-based approach generates the scenarios of the uncertainty from historical measurements [12–14]. However, this approach requires extra task such as clustering the generated scenarios.

Another challenge of ESS operation is to minimize battery degradation. Although battery price is falling, battery degradation cost is still one of the main concerns in ESS operation. Battery degradation mainly comes from charging and discharging during operation, and degradation models are based on empirical data such as depth of discharge (DoD) vs. cycle life. Rain-flow counting method was proposed to approximate total amount of battery usage in terms of DoD [15] but may not suffice because it cannot capture the state-of-charge (SoC)-dependent battery degradation. The authors in [16] proposed the concept of degradation density function to capture the battery degradation cost at each SoC, and the degradation density function is further elaborated in [17] for better function approximation.

In this paper, we propose a practical framework to manage peak load under load-forecasting error. The proposed framework has two parts: day-ahead optimization and real-time control. First, for day-ahead optimization, our method exploits dynamic programming to capture the state-dependent battery degradation. However, dynamic programming may not be as effective as linear programming in peak cut and requires an additional process to determine peak cut threshold [7]. Please note that determining the proper peak cut threshold is delicate under load uncertainty. In this regard we propose a concept of *internalized pricing* and show that the proposed method effectively cuts peak load without relying on additional process. Second, to combat against load-forecasting error, we propose a real-time control mechanism on top of the day-ahead optimization. In doing this, we investigate a concept of marginal power, which is defined as the additionally required power to follow the optimal *offline* scheduling, which is assumed to know the future load profile perfectly. Indeed, offline optimization cannot be done until the scheduling time horizon is over. Hence, we propose a learning method to estimate the marginal power from the observed forecasting errors from historical dataset. In this way we can schedule the ESS in a nearly optimal way to reduce peak power even in the presence of forecasting error while, at the same time, minimizing battery degradation and electricity cost. Finally, we verify the proposed framework by case studies. We leverage the deep learning-based short-term load-forecasting using ResNet and long short-term memory (LSTM) [18] and exploit the

sub-sampled electricity consumption data at every minute instead of the typical time interval of 15 min. Our experimental results verify that the proposed method reduces peak load by about 30% and improves the profit by almost four times compared to the case of using only day-ahead optimization.

The rest of this paper is organized as follows. In Section 2, we introduce the overall framework of the proposed system. In Section 3, we describe the internalized pricing-based day-ahead optimization. Real-time control mechanism to overcome uncertainty due to forecasting error is proposed in Section 4. Case studies are provided in Section 5, and we conclude the paper in Section 6.

2. System Overview

The proposed system has two components as shown in Figure 1. Day-ahead optimization block is used to determine the optimal battery charging/discharging scheduling based on forecasted load profiles. To alleviate the performance loss incurred from load-forecasting error, real-time control block calibrates the day-ahead scheduling. Then we estimate the marginal power for calibration using the relationship between forecasting errors and the required compensations. The estimated marginal power is then added to the day-ahead scheduling. In doing this we have two different scales of forecasting errors: 15 min interval and 1-min interval, which will be explain in detail in Section 4.2.

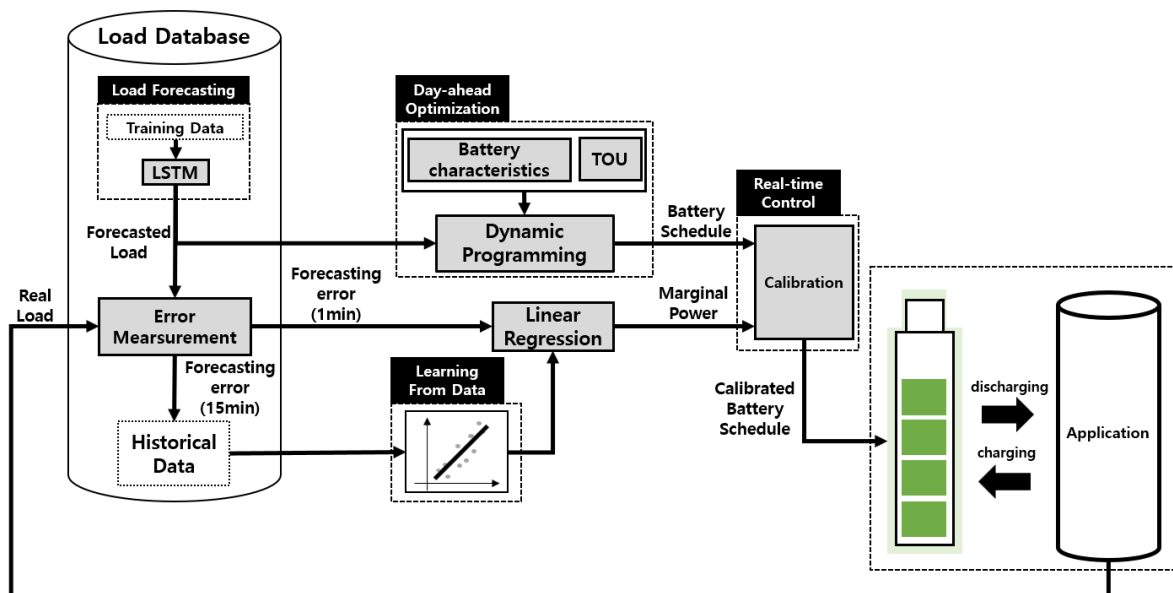


Figure 1. Overall framework of the proposed ESS scheduling.

3. Day-Ahead Optimization

In this section, we describe day-ahead optimization based on the forecasted load profile, instead of the real load profile.

3.1. Internalized Pricing-Based Approach

Let L_t denote the real load profile and \tilde{L}_t denote the day-ahead forecasted load profile at time slot $t \in \mathcal{T} = \{1, 2, \dots, T\}$ where \mathcal{T} is a scheduling horizon. Typically, scheduling time horizon is one day but can be longer depending on applications. Let p_t denote the battery power ($p_t > 0$ is charging and $p_t < 0$ is discharging) at time slot t . Then, we have the following constraint

$$\sum_{t \in \mathcal{T}} p_t = 0 \quad (1)$$

for scheduling time horizon \mathcal{T} . Let P_{\max} denote the maximum charging/discharging power of ESS, and we have

$$-P_{\max} \leq p_t \leq P_{\max} \quad \text{for } \forall t \in \mathcal{T}. \quad (2)$$

Let $s_t \in [0, 1]$ denote the battery SoC, and S_{\min} and S_{\max} denote the minimum and maximum SoC of ESS, respectively. Then,

$$S_{\min} \leq s_t \leq S_{\max} \quad \text{for } \forall t \in \mathcal{T}. \quad (3)$$

In case power injection from ESS into the grid is not allowed (e.g., under the regulation in Korea), the net power seen by the utility should be nonnegative, and thus

$$\tilde{L}_t + p_t \geq 0 \quad \text{for } \forall t \in \mathcal{T}. \quad (4)$$

Then, minimizing the total cost by using ESS can be formulated as follows [3],

$$\min_{p_t \in \mathcal{P}} \left[\left\{ \max_{t \in \mathcal{T}} (\tilde{L}_t + p_t) \right\} + \alpha \sum_{t=1}^T \mu_t (\tilde{L}_t + p_t) \Delta t \right] \quad (5)$$

where \mathcal{P} is a feasible set of battery power that satisfies (1)–(4), μ_t is an electricity price given by TOU, and α is a parameter determining the tradeoff between the peak cost that comes from $(\max_{t \in \mathcal{T}} \tilde{L}_t + p_t)$ and the energy cost. One can solve (5) using linear programming [3] unless the SoC-dependent battery degradation cost is the concern. Battery degradation, however, cannot be ignored, and to accommodate the SoC-dependent battery degradation cost, we consider the following state transition cost function from the state s_t to the state s_{t+1} :

$$C(s_t, p_t) = \mu_t (\tilde{L}_t + p_t) \Delta t + \beta E_{\max} \left| \int_{s_t}^{s_{t+1}} \omega(s) ds \right| \quad (6)$$

where β is a battery degradation coefficient [7], and $\omega(s)$ is the degradation density function that captures the state-dependent battery degradation cost. The shape of $\omega(s)$ depends on the battery characteristics and can be constructed using cycle life vs DoD data [16,17]. The next battery SoC s_{t+1} is determined by the current state s_t and the battery power p_t as follow:

$$s_{t+1} = s_t + \frac{p_t \times \Delta t}{E_{\max}} \quad (7)$$

where E_{\max} is the battery capacity. By using the transition cost function and the feasible set \mathcal{P} , we formulate the state value function as follow:

$$V(s_t) = \min_{p_t \in \mathcal{P}} \{C(s_t, p_t) + V(s_{t+1})\}. \quad (8)$$

Then, an optimal battery scheduling is determined by solving the Bellman Equation (8) [19]. However, the subtlety lies in that the solution based on dynamic programming does not consider the cost incurred by the peak load. A simple method is to impose peak power threshold by preventing abrupt state transition [7]. However, determining a proper threshold requires additional process, which might be vulnerable to load-forecasting error. To overcome this limitation, we propose a new cost function by adding a *penalty term* $\gamma(\tilde{L}_t + p_t)$ into μ_t such as

$$\tilde{C}(s_t, p_t) = \left(\mu_t + \gamma(\tilde{L}_t + p_t) \right) (\tilde{L}_t + p_t) \Delta t + \beta E_{\max} \left| \int_{s_t}^{s_{t+1}} \omega(s) ds \right| \quad (9)$$

where γ is a weight parameter that determines the cost of peak load. Please note that (9) is not restricted to the peak management under KCI tariff but can be applicable to other tariffs by properly selecting μ_t and γ . Then we have a new Bellman equation as follows:

$$\tilde{V}(s_t) = \min_{p_t \in \mathcal{P}} \{ \tilde{C}(s_t, p_t) + \tilde{V}(s_{t+1}) \}. \tag{10}$$

The intuition of constructing (9) is such that TOU is replaced by a user-defined TOU which has high price when the net load (load plus battery power) becomes high.

It turns out that slight tweaking the cost function using the *internalized pricing* dramatically contributes to reducing the peak. Traditional peak minimization of (5) when $\alpha = 0$ is the min-max operation (or L_∞ norm minimization) of $\tilde{L}_t + p_t, \forall t \in \mathcal{T}$ and can be solved by using linear programming. However, it cannot consider the state-dependent battery degradation and can be vulnerable to load-forecasting error. Finally, the day-ahead optimal battery power \tilde{p}_t is given by

$$\tilde{p}_t = \arg \min_{p_t \in \mathcal{P}} \{ \tilde{C}(s_t, p_t) + \tilde{V}(s_{t+1}) \}. \tag{11}$$

3.2. Implication of Internalized Pricing

The implication of solving (10)–(11) using the internalized pricing is as follows. When $\beta = 0$ in (9) and γ is sufficiently large, both of battery degradation and the energy cost from TOU are ignored and solving (11) leads to minimizing $\sum_{t \in \mathcal{T}} (\tilde{L}_t + p_t)^2$, i.e., L_2 norm minimization, instead of L_∞ norm minimization, of $\tilde{L}_t + p_t, \forall t \in \mathcal{T}$. Now we motivate the use of L_2 norm minimization for peak management. For simple illustration we consider a vector $\mathbf{x} = (x_1, x_2)$ in some feasible region $\mathcal{S} \subset \mathcal{R}^2$.

Let \mathbf{x}^∞ be the solution of $\min \|\mathbf{x}\|_\infty$ subject to $\mathbf{x} \in \mathcal{S}$ and \mathbf{x}^* be the solution of $\min \|\mathbf{x}\|_2$ subject to $\mathbf{x} \in \mathcal{S}$. In Figure 2, we plot the feasible region \mathcal{S} and the contours that have the same L_2 norm (dash) and L_∞ norm (dash dot). As illustrated in Figure 2a, the solutions of L_2 norm minimization and L_∞ norm minimization can be identical. That is, in this case, using L_2 method has the same peak power as L_∞ method. However, in Figure 2b, the solutions of L_2 norm minimization and L_∞ norm minimization can be different, i.e., L_2 norm minimization has higher peak power than L_∞ minimization.

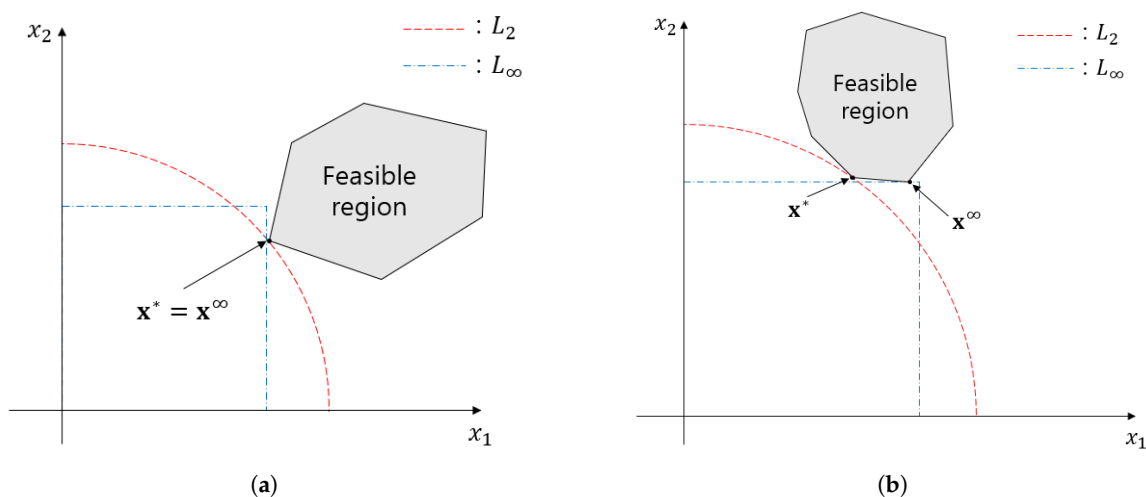


Figure 2. (a) L_2 norm minimization (\mathbf{x}^*) and L_∞ norm minimization (\mathbf{x}^∞) have the same solution. (b) L_2 norm minimization (\mathbf{x}^*) and L_∞ norm minimization (\mathbf{x}^∞) have different solutions.

Back to our problem, \mathbf{x} lies in \mathcal{P} , which is determined from the constraints of battery power (1)–(4), and it is of interest to know under which circumstance L_2 norm minimization is sufficient to minimize the peak load. The following proposition summarizes the result in terms of the battery capacity \bar{E}_{\max} , and the initial SoC s_0 .

Proposition 1 (Sufficient condition of solution equivalence). Given the scheduling time horizon \mathcal{T} , if the battery capacity \bar{E}_{\max} and the initial SoC s_0 are given by

$$\bar{E}_{\max} = \frac{\max_{\tau \in \mathcal{T}} \sum_{t=1}^{\tau} p_t \Delta t - \min_{\tau \in \mathcal{T}} \sum_{t=1}^{\tau} p_t \Delta t}{S_{\max} - S_{\min}}, \quad (12)$$

and

$$s_0 = S_{\max} - \frac{\max_{\tau} \sum_{t=1}^{\tau} p_t \Delta t}{\bar{E}_{\max}}, \quad (13)$$

L_2 norm minimization has the same solution of L_{∞} norm minimization.

Proof. Let L_{avg} denote the average load in the scheduling horizon \mathcal{T} . The battery power to make the net load equal to the average load is

$$p_t = L_{avg} - L_t. \quad (14)$$

Since p_t is provided by the battery, the summation of (14) over time is the energy stored in the battery. Thus, we have

$$\bar{E}_{\max}(S_{\max} - s_0) = \max_{\tau \in \mathcal{T}} \sum_{t=1}^{\tau} p_t \Delta t \geq 0, \quad (15)$$

and

$$\bar{E}_{\max}(S_{\min} - s_0) = \min_{\tau \in \mathcal{T}} \sum_{t=1}^{\tau} p_t \Delta t \leq 0. \quad (16)$$

By subtracting (16) from (15), \bar{E}_{\max} is given by

$$\bar{E}_{\max} = \frac{\max_{\tau} \sum_{t=1}^{\tau} p_t \Delta t - \min_{\tau} \sum_{t=1}^{\tau} p_t \Delta t}{S_{\max} - S_{\min}}. \quad (17)$$

In addition, s_0 can be obtained by inserting \bar{E}_{\max} into (15), which completes the proof. \square

Example 1. Figure 3 compares two methods for various battery capacities. In our case, surprisingly, the peak power of L_2 norm minimization is same to that of L_{∞} norm minimization for all battery capacities. This is possible because Proposition 1 is the sufficient condition that L_2 minimization equals to L_{∞} minimization.

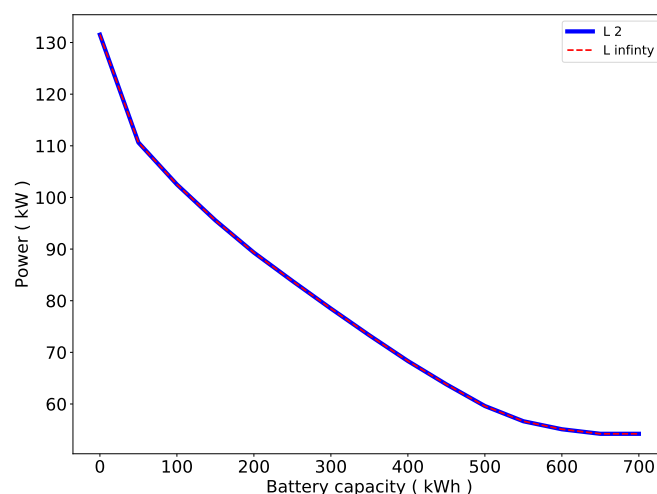


Figure 3. Comparing L_2 and L_{∞} norm minimization in terms of peak management.

4. Real-Time Control Method

4.1. The Proposed Marginal Power

So far we have discussed the day-ahead optimization based on the forecasted load profile \tilde{L}_t . However, load-forecasting inevitably has error, and thus day-ahead optimization cannot be optimal for real load profile L_t ; the optimal scheduling for the real load profile can be done only after the scheduling time horizon \mathcal{T} is over, and thus it is indeed *offline scheduling*. Since day-ahead optimization cannot be the same to the offline optimization, additional mechanism is required to calibrate it. If one can estimate the power required to mimic the offline optimization by observing the load-forecasting error for some past period, real-time calibration can be possible. In this regard, we propose the marginal power, denoted by m_t , as follow:

$$m_t = p_t^* - \tilde{p}_t \quad (18)$$

where p_t^* is the battery power obtained by the offline optimization based on the real load profile L_t . Hence, day-ahead scheduled battery power plus the marginal power can be equal to the offline optimal battery power. Let e_t denote the load-forecasting error:

$$e_t := L_t - \tilde{L}_t. \quad (19)$$

Then, based on the offline scheduling, we investigate the relationship between the load-forecasting error e_t and the offline marginal power m_t . For illustrative purpose, we synthesize a forecasted load profile \tilde{L}_t by simply adding filtered Gaussian noise to L_t . In Section 5, we will use LSTM-based load-forecasting to validate the proposed approach. Surprisingly, as can be seen in Figure 4, offline marginal power turns out to have a strong linear relation with load-forecasting error.

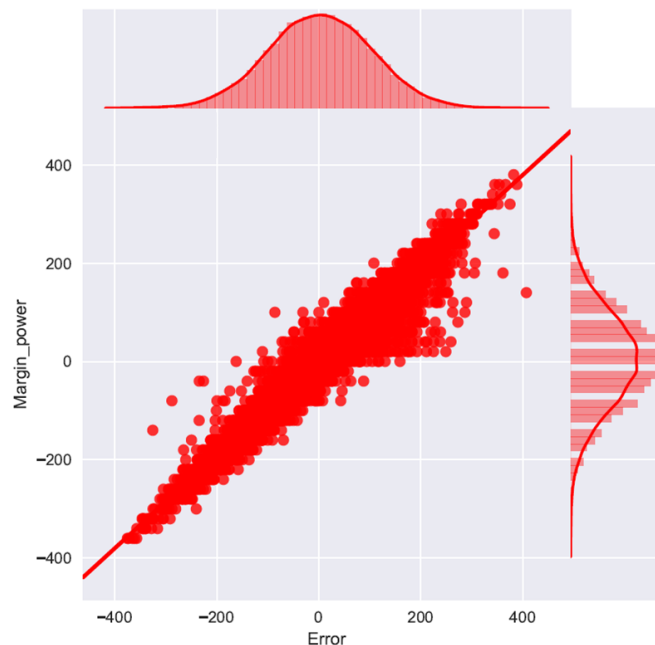


Figure 4. Relationship between marginal power and load-forecasting error.

By applying linear regression, we can estimate the marginal power from the load-forecasting error as follows:

$$\hat{m}_t = \theta_0 + \theta_1 e_t \quad (20)$$

where \hat{m}_t is the estimated marginal power, θ_0 is a bias term and θ_1 is the slope; θ_0 and θ_1 should be learned from historical dataset. The calibrated real-time battery power \hat{p}_t is then given by

$$\hat{p}_t = \tilde{p}_t + \hat{m}_t. \quad (21)$$

One subtlety still lies in that, however, the forecasting error e_t can be measured *only after* time slot t ends and the real load profile L_t is observed.

4.2. Leveraging Sub-Time Slot for Marginal Power Allocation

Recall that the load is measured every time slot such as 15 min. However, if the load can be measured more frequently, e.g., in every minute, which is much shorter than the duration of one time slot, we can reduce the delay to measure the load-forecasting error, and thus can allocate the estimated marginal power effectively. Indeed, there are commercially available smart meters that can sense the power consumption very frequently, e.g., every sub-second [20]. Hence, the estimated marginal power per sub-time slot is allocated in the *next* sub-time slot. The delayed allocation of one sub-time slot is allowed as long as it belongs to the original time slot. Figure 5 illustrates how the marginal power can be estimated and allocated per sub-time slot. In this way, the proposed method performs seemingly real-time calibration.

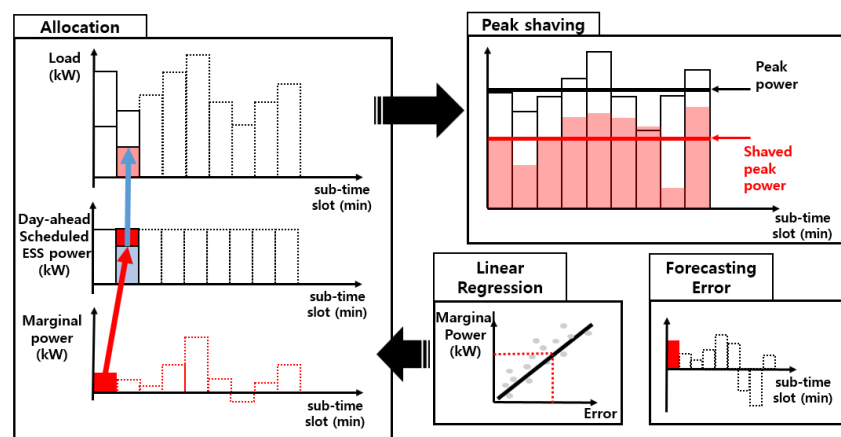


Figure 5. Real-time control technique in sub-time slots.

5. Case Studies

In this section, we provide the experimental results of the proposed system using the real load profiles measured per sub-time slot. The time slot duration is 15 min, and the sub-time slot duration is 1 min. Since both fully charged and discharged SoC impairs the battery health, the minimum and the maximum of SoC are set as 10% and 90%, respectively. Other parameters for the experiments are summarized in Table 1.

Table 1. Simulation parameters.

Parameters	Symbols	Value (Unit)
Time slot duration	Δt	15 min
Sub-time slot duration		1 min
Battery unit price		150 (\$/kWh)
Battery capacity	\bar{E}_{\max}	600 (kWh)
Maximum battery power	P_{\max}	100 (kW)
Initial SoC	s_0	80 (%)
Minimum, Maximum SoC	s_{\min}, s_{\max}	10, 90 (%)
Degradation weight	β	0.5
Peak load weight	γ	0.277 (\$/kW)

Since load-forecasting is essential, we use the ResNet/LSTM-based load-forecasting as in our previous work [18]. The load-forecasting is done for every time slot as typically used in practice. The real load profiles and the forecasted load profiles are shown in Figure 6, and the original peak load is 131.5 kW. We use the load profiles of manufacturing facility, and 185 days are used for training/validation to forecast the load profiles from March 1st to 20th. One may think this data is not sufficient for reliable forecasting. However, our intension is not to accurately forecast load profiles but test our proposed algorithm under forecasting errors. Load-forecasting itself is not the scope of this paper, and please refer to [18] for the details of load-forecasting. Indeed, the proposed method can be combined with other load-forecasting techniques and would be more effective if forecasting is not accurate. Figure 7 shows the probability density function of forecasting error; the mean of error is almost zero, and the mean absolute percentage error (MAPE) is 10%. As can be seen in Figures 6 and 7, load-forecasting is not quite accurate sometimes, which is the motivation of our work. For example, in the 11th day (around time slot 1000), the forecasted load is very low, but the real load is unexpectedly high. Figure 8 is the TOU price under the KCI tariff in March. Using the parameters and the load profiles introduced so far, the proposed method calculates the optimal battery schedule considering TOU, peak load, and battery degradation under uncertainty.

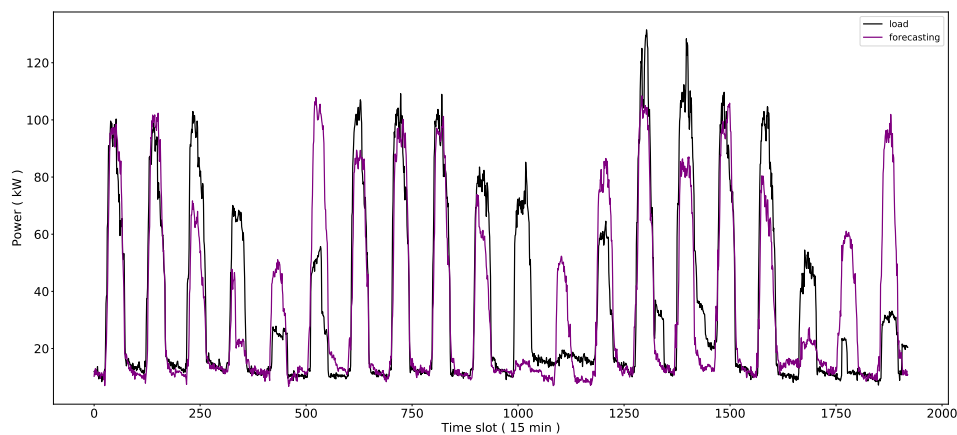


Figure 6. The real and forecasted load profiles using ResNet/LSTM.

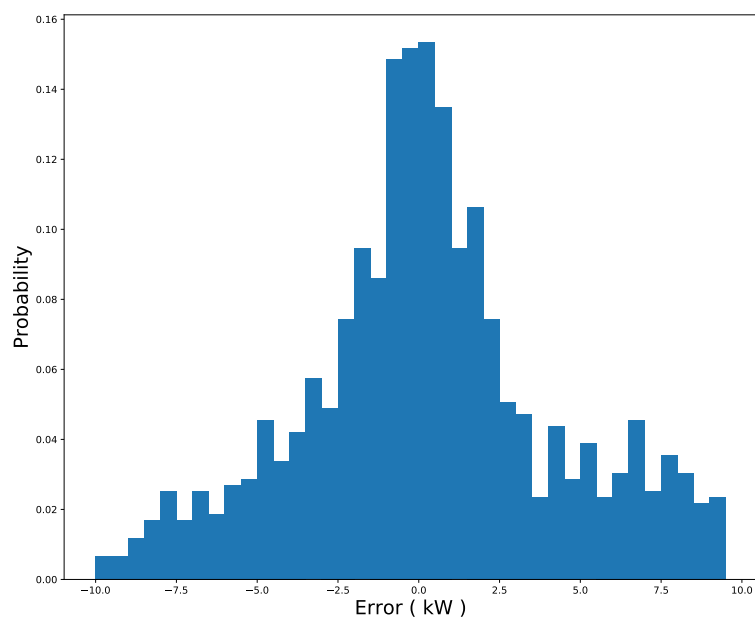


Figure 7. Probability density function of load-forecasting error.

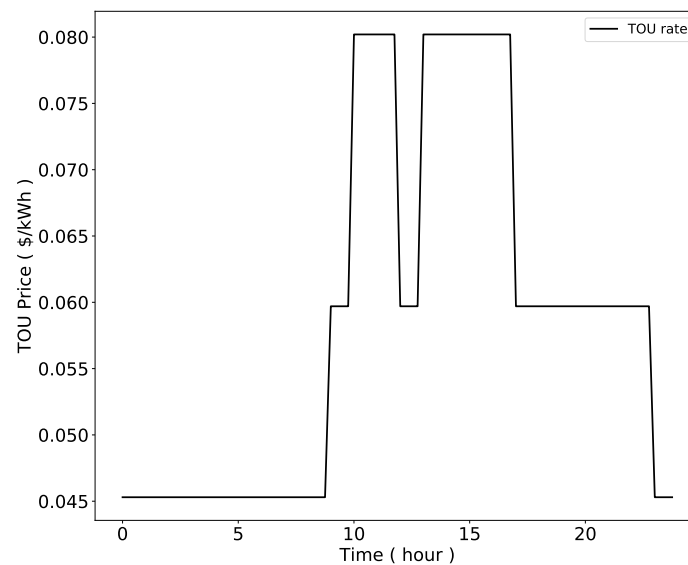


Figure 8. TOU Price.

5.1. Single Day Operation

The result for single day operation is presented in Figure 9. As explained in Section 4.1, we estimate the marginal power from the forecasting error using linear regression as shown in Figure 9a. For linear regression we use the data from the same day of one week ago considering the weekly periodicity of load profiles. As can be seen in Figure 9a, the marginal power is well estimated by linear regression.

In Figure 9b we present the load profiles based on various ESS schedulings. We see that from time slots 30 to 70, the forecasted load profile (purple line) deviates from the real load profile (black line), and consequently the result of day-ahead optimization (green line) is quite different from the offline battery scheduling (red line). The original peak load is 109.2 kW, and the day-ahead optimization reduces it to 87.4 kW, i.e., 20.0% of peak reduction. By contrast, the proposed method achieves 60.1 kW of peak power, which is 31% of improvement from the day-ahead optimization. Please note that the peak power of offline scheduling is 55.7 kW, so the proposed method is almost as good as the optimal result. Table 2 summarizes the cost/profit analysis. The proposed technique earns \$419, which is more than double compared to the profit of the day-ahead optimization, and is also close to the offline optimal profit of \$452.6.

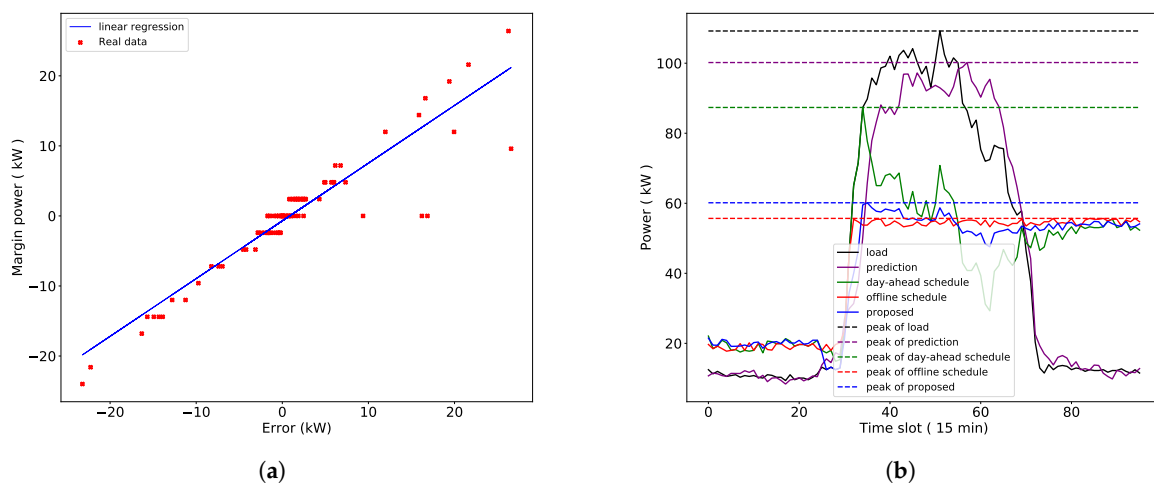


Figure 9. Result of single day operation. (a) Forecasting error and marginal power, (b) Load profiles obtained by various ESS schedulings.

Table 2. Cost and profit analysis of single day operation.

Feature	Without ESS	Day-Ahead	Proposed	Offline
Peak power (kW)	109.2	87.4	60.1	55.7
Base cost (\$)	908.5	726.8	500.4	463.3
Cost by TOU (\$)	279.2	255.1	254.7	257.8
Battery degradation cost (\$)	-	13.3	13.6	14.0
Total cost (\$)	1187.7	995.3	768.7	735.1
Profit (\$)	-	192.4	419.0	452.6

5.2. Robustness of the Proposed Method

Next we investigate the robustness of the proposed method. Specifically, we consider the case when the forecasted load profile has time misalignment, which may happen when the operation of manufacturing facilities unexpectedly shifts in time. Figure 10a shows the relationship between the load-forecasting error and the marginal power, and the marginal power can be well estimated from the load-forecasting error. Figure 10b shows the load profiles based on various ESS schedulings. In the case of day-ahead optimization, the failure of load-forecasting results in very unwanted load profile where the peak power is not reduced at all. Indeed, as seen in Table 3, the peak power slightly increases from 109.2 kW to 109.4 kW, and ESS becomes of no use. By contrast, the proposed method reduces the peak power to 67.2 kW while the optimal peak power from offline scheduling is 55.7 kW. Thus, the proposed method works well even under the unexpected load shift in time. Furthermore, the profit earned by the proposed method is \$368.6, which recovers 81.4% of the profit from the offline scheduling.

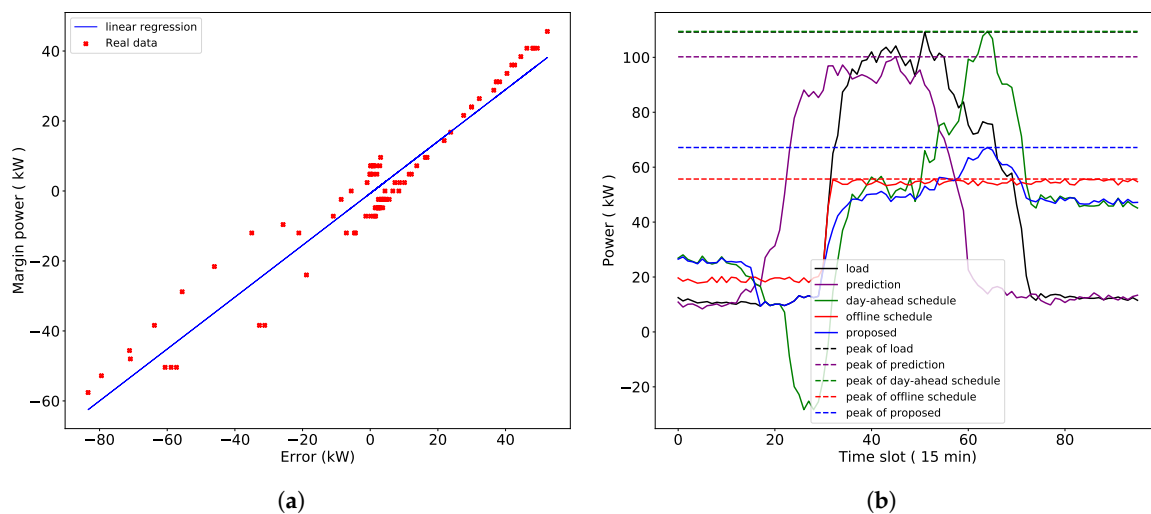


Figure 10. Result of single day operation with unexpected load shifts in hours. (a) Forecasting error and marginal power, (b) Load profiles obtained by various ESS schedulings.

Table 3. Cost and profit analysis under unexpected load shift in time.

Feature	Without ESS	Day-Ahead	Proposed	Offline
Peak power (kW)	109.2	109.4	67.2	55.7
Base cost (\$)	908.5	910.5	558.8	463.3
Cost by TOU (\$)	279.2	275.2	247.5	257.8
Battery degradation cost (\$)	-	15.4	12.9	14.0
Total cost (\$)	1187.7	1202.1	819.1	735.1
Profit (\$)	-	-14.4	368.6	452.6

5.3. Multiple Day Operation

Finally, we apply the proposed method for multiple day operation. As in the case of single day operation, we use the data from the same day of one week ago for linear regression. In single day operation, the starting and the ending SoC are both set as s_0 for all three methods as shown in Table 1. This still holds for day-ahead optimization and offline optimization because the sum of battery power in one day is zero. In the case of the proposed method, however, the battery power is adjusted by the marginal power, whose sum in one day may not be zero. Hence, we cannot enforce s_0 for both the starting SoC and the ending SoC. Thus, we set the target SoC as s_0 only at the end of each day. As can be seen in Figure 11 and Table 4, the proposed method outperforms the day-ahead method and closely follows the offline optimization. The original peak load is 131.5 kW without using ESS, and the day-ahead method reduces the peak to 97.2 kW while the proposed method further reduces it to 69.0 kW, which is also comparable to the offline optimal peak of 55 kW. It should be noted that the scheduling horizon is just one day for the proposed method. Thus, the proposed method for multiple days is applied by repeating the scheduling horizon. In the case of the offline optimization, however, the scheduling horizon covers the whole days to compute the theoretical minimum bound. In terms of profit for the proposed method, the battery degradation cost is \$141.4, and the profit is \$595.1. By contrast, the day-ahead method has only \$151.7 of profit. The result for a longer period of operation can be obtained when more data measured in sub-time slots become available.

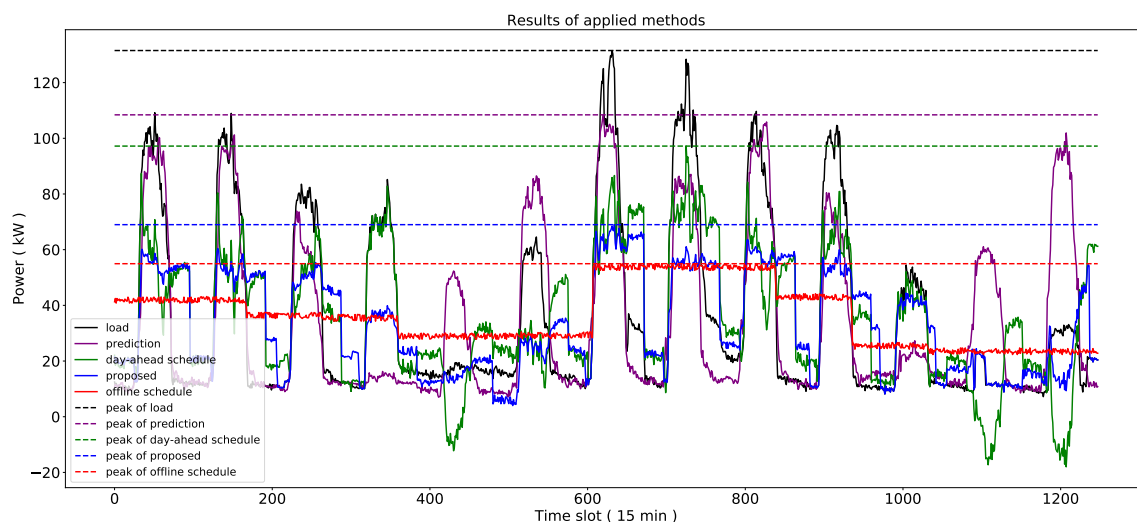


Figure 11. Result of multiple day operation.

Table 4. Results of the proposed method for multiple day operation.

Feature	Without ESS	Day-Ahead	Proposed	Offline
Peak power (kW)	131.5	97.2	69.0	55.0
Base cost (\$)	1094.2	808.7	573.9	457.3
Cost by TOU (\$)	2963.5	2916.0	2747.3	2673.8
Battery degradation cost (\$)	-	181.3	141.4	153.5
Total cost (\$)	4057.7	3906.0	3462.6	3284.5
Profit (\$)	-	151.7	595.1	773.2

6. Conclusions

In this paper, we proposed a two-phase approach to minimize the total cost including the peak cost, the energy usage cost from TOU and the battery degradation cost. The first phase is the day-ahead optimization based on the forecasted load profile and exploits the concept of internalized pricing, which enables us to effectively manage the peak load without bothering to select the peak cut threshold. The proposed method is based on dynamic programming and thus can accommodate the

SoC-dependent battery degradation cost. However, the subtlety of managing peak power comes from the load-forecasting error. Hence, in the second phase we proposed a real-time control mechanism based on the marginal power to compensate the performance loss incurred by the load-forecasting error. The marginal power is computed from the load-forecasting error by using linear regression and allocated in sub-time slot, e.g., every one minute. Case studies with real load profiles verified that the proposed method substantially improves the day-ahead method; under load-forecasting uncertainty, the peak power using the proposed method is only 22.4% higher than that of the offline optimal scheduling while the day-ahead optimization has 76.8% higher peak power than the offline optimal power. In terms of profit, the proposed method achieves 77.0% of the offline optimal profit while the day-ahead method only earns 19.6% of the offline optimal profit, which shows that the proposed method outperforms the day-ahead optimization under uncertainty.

Author Contributions: M.K. analyzed the day-ahead optimization using internalized pricing, wrote many parts of this paper and performed numerical simulations. K.K. conceived the idea of internalized pricing and the marginal power. H.C. performed load forecasting using ResNet/LSTM. S.L. was in charge of analyzing the real load profiles measured in sub-time slot using the ENERTALK sensor of Encored Technologies. H.K. led the entire project and research.

Funding: This work was supported by the Korea Institute of Energy Technology Evaluation and Planning(KETEP) and the Ministry of Trade, Industry & Energy(MOTIE) of the Republic of Korea. (No. 2016121020036, No. 20172010000370).

Conflicts of Interest: The authors declare no conflict of interest.

References

1. Oudalov, A.; Chartouni, D.; Ohler, C. Optimizing a battery energy storage system for primary frequency control. *IEEE Trans. Power Syst.* **2007**, *22*, 1259–1266. [[CrossRef](#)]
2. Cai, Y.; Huang, G.; Yang, Z.; Tan, Q. Identification of optimal strategies for energy management systems planning under multiple uncertainties. *Appl. Energy* **2009**, *86*, 480–495. [[CrossRef](#)]
3. Kim, J.; Choi, Y.; Ryu, S.; Kim, H. Robust Operation of Energy Storage System with Uncertain Load Profiles. *Energies* **2017**, *10*, 416. [[CrossRef](#)]
4. Parisio, A.; Glielmo, L. Energy efficient microgrid management using model predictive control. In Proceedings of the 2011 50th IEEE Conference on Decision and Control and European Control Conference, Orlando, FL, USA, 12–15 December 2011; pp. 5449–5454.
5. Uddin, M.; Romlie, M.F.; Abdullah, M.F.; Halim, S.A.; Kwang, T.C.; Abu Bakar, A.H. A review on peak load shaving strategies. *Renew. Sustain. Energy Rev.* **2018**, *82*, 3323–3332. [[CrossRef](#)]
6. Sun, S.; Dong, M.; Liang, B. Joint supply, demand, and energy storage management towards microgrid cost minimization. In Proceedings of the 2014 IEEE International Conference on Smart Grid Communications (SmartGridComm), Venice, Italy, 3–6 November 2014; pp. 109–114.
7. Choi, Y.; Kim, H. Optimal scheduling of energy storage system for self-sustainable base station operation considering battery wear-out cost. *Energies* **2016**, *9*, 462. [[CrossRef](#)]
8. Kodaira, D.; Yu, B.; Jung, W.; Han, S. Optimized ESS Operation for Peak Shaving based on Probabilistic Load Prediction. In Proceedings of the 2018 IEEE Innovative Smart Grid Technologies-Asia (ISGT Asia), Singapore, 22–25 May 2018; pp. 1199–1203.
9. Even, A.; Neyens, J.; Demouselle, A. Peak shaving with batteries. In Proceedings of the 12th International Conference on Electricity Distribution, Birmingham, UK, 17–21 May 1993; pp. 5–17.
10. Liu, J.; Chen, H.; Zhang, W.; Yurkovich, B.; Rizzoni, G. Energy management problems under uncertainties for grid-connected microgrids: A chance constrained programming approach. *IEEE Trans. Smart Grid* **2017**, *8*, 2585–2596. [[CrossRef](#)]
11. Li, Y.; Yang, Z.; Li, G.; Zhao, D.; Tian, W. Optimal scheduling of an isolated microgrid with battery storage considering load and renewable generation uncertainties. *IEEE Trans. Ind. Electron.* **2019**, *66*, 1565–1575. [[CrossRef](#)]
12. Stai, E.; Reyes-Chamorro, L.; Sossan, F.; Le Boudec, J.Y.; Paolone, M. Dispatching stochastic heterogeneous resources accounting for grid and battery losses. *IEEE Trans. Smart Grid* **2018**, *9*, 6522–6539. [[CrossRef](#)]

13. Parvizimosaed, M.; Farmani, F.; Monsef, H.; Rahimi-Kian, A. A multi-stage Smart Energy Management System under multiple uncertainties: A data mining approach. *Renew. Energy* **2017**, *102*, 178–189. [[CrossRef](#)]
14. Nouri, A.; Soroudi, A.; Keane, A. Strategic Scheduling in Smart Grids. In Proceedings of the 2018 IEEE International Conference on Environment and Electrical Engineering and 2018 IEEE Industrial and Commercial Power Systems Europe (EEEIC/I&CPS Europe), Palermo, Italy, 12–15 June 2018; pp. 1–5.
15. Gee, A.M.; Robinson, F.V.; Dunn, R.W. Analysis of battery lifetime extension in a small-scale wind-energy system using supercapacitors. *IEEE Trans. Energy Convers.* **2013**, *28*, 24–33. [[CrossRef](#)]
16. Han, S.; Han, S.; Aki, H. A practical battery wear model for electric vehicle charging applications. *Appl. Energy* **2014**, *113*, 1100–1108. [[CrossRef](#)]
17. Kim, K.; Choi, Y.; Kim, H. Data-driven battery degradation model leveraging average degradation function fitting. *Electron. Lett.* **2016**, *53*, 102–104. [[CrossRef](#)]
18. Choi, H.; Ryu, S.; Kim, H. Short-Term Load Forecasting based on ResNet and LSTM. In Proceedings of the 2018 IEEE International Conference on Communications, Control, and Computing Technologies for Smart Grids (SmartGridComm), Aalborg, Denmark, 29–31 October 2018; pp. 1–6.
19. Levron, Y.; Guerrero, J.M.; Beck, Y. Optimal power flow in microgrids with energy storage. *IEEE Trans. Power Syst.* **2013**, *28*, 3226–3234. [[CrossRef](#)]
20. EnerTalk. Available online: <https://www.enertalk.com> (accessed on 26 February 2019).



© 2019 by the authors. Licensee MDPI, Basel, Switzerland. This article is an open access article distributed under the terms and conditions of the Creative Commons Attribution (CC BY) license (<http://creativecommons.org/licenses/by/4.0/>).